



ARL-TR-7258 • APR 2015



US Army Research Laboratory

Optimization of Thick Negative Photoresist for Fabrication of Interdigitated Capacitor Structures

by Erik Enriquez, D Shreiber, E Ngo, M Ivill, SG Hirsch,
C Hubbard, and MW Cole

Approved for public release; distribution is unlimited.

NOTICES

Disclaimers

The findings in this report are not to be construed as an official Department of the Army position unless so designated by other authorized documents.

Citation of manufacturer's or trade names does not constitute an official endorsement or approval of the use thereof.

Destroy this report when it is no longer needed. Do not return it to the originator.



Optimization of Thick Negative Photoresist for Fabrication of Interdigitated Capacitor Structures

**by Erik Enriquez, D Shreiber, E Ngo, M Ivill, SG Hirsch,
C Hubbard, and MW Cole**
Weapons and Materials Research Directorate, ARL

REPORT DOCUMENTATION PAGE				Form Approved OMB No. 0704-0188	
<p>Public reporting burden for this collection of information is estimated to average 1 hour per response, including the time for reviewing instructions, searching existing data sources, gathering and maintaining the data needed, and completing and reviewing the collection information. Send comments regarding this burden estimate or any other aspect of this collection of information, including suggestions for reducing the burden, to Department of Defense, Washington Headquarters Services, Directorate for Information Operations and Reports (0704-0188), 1215 Jefferson Davis Highway, Suite 1204, Arlington, VA 22202-4302. Respondents should be aware that notwithstanding any other provision of law, no person shall be subject to any penalty for failing to comply with a collection of information if it does not display a currently valid OMB control number.</p> <p>PLEASE DO NOT RETURN YOUR FORM TO THE ABOVE ADDRESS.</p>					
1. REPORT DATE (DD-MM-YYYY) April 2015		2. REPORT TYPE Final		3. DATES COVERED (From - To) 1 May–30 November 2014	
4. TITLE AND SUBTITLE Optimization of Thick Negative Photoresist for Fabrication of Interdigitated Capacitor Structures				5a. CONTRACT NUMBER	
				5b. GRANT NUMBER	
				5c. PROGRAM ELEMENT NUMBER	
6. AUTHOR(S) Erik Enriquez, D Shreiber, E Ngo, M Ivill, SG Hirsch, C Hubbard, and MW Cole				5d. PROJECT NUMBER	
				5e. TASK NUMBER	
				5f. WORK UNIT NUMBER	
7. PERFORMING ORGANIZATION NAME(S) AND ADDRESS(ES) US Army Research Laboratory ATTN: RDRL-WMM-E Aberdeen Proving Ground, MD 21005-5069				8. PERFORMING ORGANIZATION REPORT NUMBER ARL-TR-7258	
9. SPONSORING/MONITORING AGENCY NAME(S) AND ADDRESS(ES)				10. SPONSOR/MONITOR'S ACRONYM(S)	
				11. SPONSOR/MONITOR'S REPORT NUMBER(S)	
12. DISTRIBUTION/AVAILABILITY STATEMENT Approved for public release; distribution is unlimited.					
13. SUPPLEMENTARY NOTES All correspondence should be directed to melanie.w.cole.civ@mail.mil.					
14. ABSTRACT Investigations were conducted in the optimization of a lift-off photolithography technique using thick negative photoresist (PR) NR9-8000 to achieve and optimize micron-scale interdigitated capacitor (IDC) structures by lift-off process for use in high-frequency electrical characterization measurements. Target feature resolution was in the range of 3–20 µm, with PR thickness in the range of 6–20 µm. Systematic deviations were made from manufacturer-recommended PR processing conditions to investigate a processing-structure relationship for optimizing of IDC fabrication including PR response to manipulation of substrate material, spin-speed, postexposure bake, exposure dose, and development process conditions. Postexposure bake temperature was found to be the most sensitive and critical parameter for the optimization of PR structures.					
15. SUBJECT TERMS lithography, IDC, microwave characterization, photoresist					
16. SECURITY CLASSIFICATION OF:			17. LIMITATION OF ABSTRACT UU	18. NUMBER OF PAGES 24	19a. NAME OF RESPONSIBLE PERSON MW Cole
a. REPORT Unclassified	b. ABSTRACT Unclassified	c. THIS PAGE Unclassified			19b. TELEPHONE NUMBER (Include area code) 410-306-0747

Contents

List of Figures	iv
List of Tables	iv
Acknowledgments	v
1. Introduction	1
1.1 Photolithography	1
1.2 Coating and Removal Techniques	3
1.3 Processing Challenges	5
2. Methods	5
2.1 Spin-Coat Study	6
2.2 Postexposure Bake Study	7
2.3 Development Time Study	7
2.4 Coating by Electron-Beam and DC Sputter Deposition	8
3. Results and Discussion	8
3.1 Spin-Coat Study Results	8
3.2 Postexposure Bake Study Results	9
3.3 Development Time Study Results	9
3.4 Coating by E-Beam and DC Sputter Deposition Results	11
4. Conclusions	12
5. References	13
List of Symbols, Abbreviations, and Acronyms	14
Distribution List	15

List of Figures

Fig. 1	Photolithography process used with negative-tone PR chemical Futurrex NR9-8000: 1) spin-coat PR, 2) soft-bake, 3) UV exposure, 4) postexposure bake, 5) developer solution immersion, and 6) N ₂ dry	1
Fig. 2	a) Positive and b) negative PR structures during exposure and after development	2
Fig. 3	Comparison of a) lift-off and b) dry-etching PR removal techniques. While lift-off uses solution to remove PR from the substrate, etching techniques dissolve a uniform top layer of material, both PR and metal. 3	3
Fig. 4	Comparison of a) undercut sidewall profile that promotes coating discontinuities for easier lift-off and b) overcut sidewall profile	5
Fig. 5	a) Comb pattern and b) IDC pattern mask schematics with feature dimensions	6
Fig. 6	Profilometry measurement setup for thickness measurement of as-applied PR layer prior to exposure and development processing: 1) apply Kapton tape, 2) spin-coat PR and soft-bake, 3) remove Kapton tape, and 4) measure step height	7
Fig. 7	PR profile after postexposure bake processing from room temperature to 110 °C	9
Fig. 8	Cross-section SEM micrographs of samples processed with 34-, 40-, and 46-s developer immersion durations	10
Fig. 9	SEM cross-section of PR structures after coating with 2 µm of Cu: a) e-beam deposition and b) sputter deposition.....	11
Fig. 10	Optical microscopy of Cu structures after lift-off removal of PR for a) comb pattern by e-beam, b) comb pattern by DC sputtering, c) IDC pattern by e-beam, and d) IDC pattern by DC sputtering	12

List of Tables

Table 1.	Expected PR thicknesses vs. measured thickness values after soft-bake and after development.....	8
Table 2	Achieved feature dimensions for comb-mask pattern with variation of development duration.....	10

Acknowledgments

The lead author of this manuscript, Erik Enriquez, would like to thank the US Army Research Laboratory and the dedicated individuals of the Integrated Electromagnetic Materials Research Team for making this research possible. I would especially like to thank MW Cole for her mentorship, inspiration, and continual help and for her fruitful and thoughtful contributions that enabled this research.

INTENTIONALLY LEFT BLANK.

1. Introduction

1.1 Photolithography

Photolithography is a technique primarily used for patterning of features, down to micron and submicron feature scales, in electronic device circuit applications.^{1,2} Photolithography uses ultraviolet (UV) light-sensitive chemical solutions to transfer a solid pattern onto a substrate. This solid pattern can then be filled in or coated with layers of desired materials, adding more elements of manufacture control to a device design. There are many variations of photolithography processes that are tailored for use in a range of processing temperature conditions, material compatibility, wavelength, and resolution specifications, as well as removal techniques, all of which have specific processing methods. The latest development of interdigitated capacitor (IDC) structures presented in this research is the Futurrex NR9-8000, which is a negative-tone photoresist (PR) designed for use in thick film (6- to 100- μm) applications. The process, presented in Fig. 1, begins with application of PR material on a substrate by spin-coat method. The spinning speed and duration dictates the PR layer thickness.

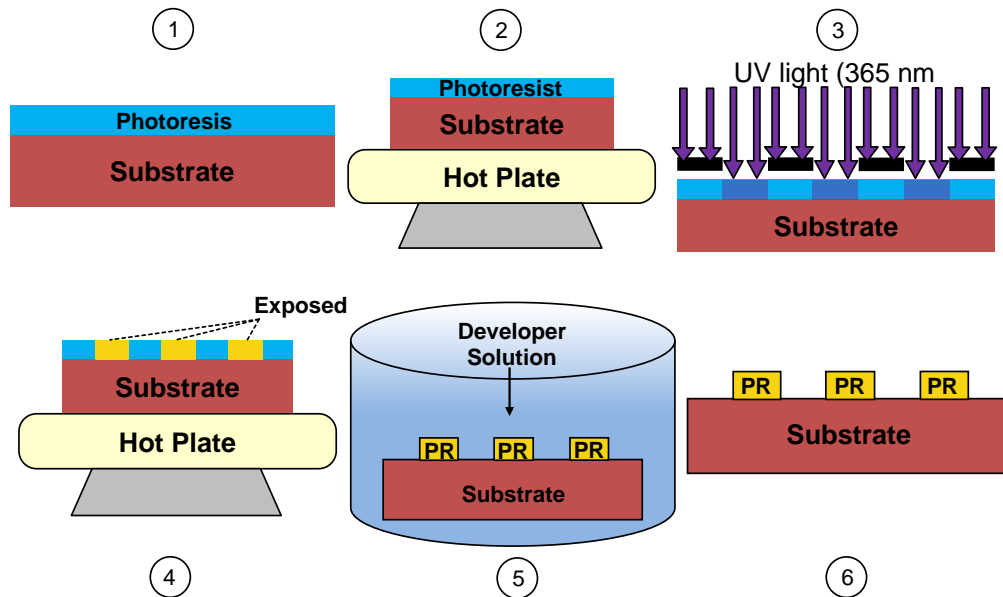


Fig. 1 Photolithography process used with negative-tone PR chemical Futurrex NR9-8000: 1) spin-coat PR, 2) soft-bake, 3) UV exposure, 4) postexposure bake, 5) developer solution immersion, and 6) N₂ dry

After the spin-coat application, a soft-bake step is required to evaporate solvents and harden the PR layer. This can be performed either by hot plate or oven heating, and also serves as a stabilizing action for the PR chemicals. Prior to this step, some PR chemicals are highly sensitive to ambient temperature and humidity conditions, and manufacturer recommendations are usually made to ensure appropriate processing results. The exposure step uses a UV light source and mask structure that mirrors the desired pattern to be transferred to selectively expose areas of the PR chemical layer. Here there are 2 main types of PR materials to be considered: positive- and negative-tone PRs. Positive PRs refer to a pattern transfer that is identical to the mask that is used during exposure, in contrast with negative PRs, which produce a PR pattern in the negative image of the mask used during exposure. An illustration of positive and negative PRs is given in Fig. 2.

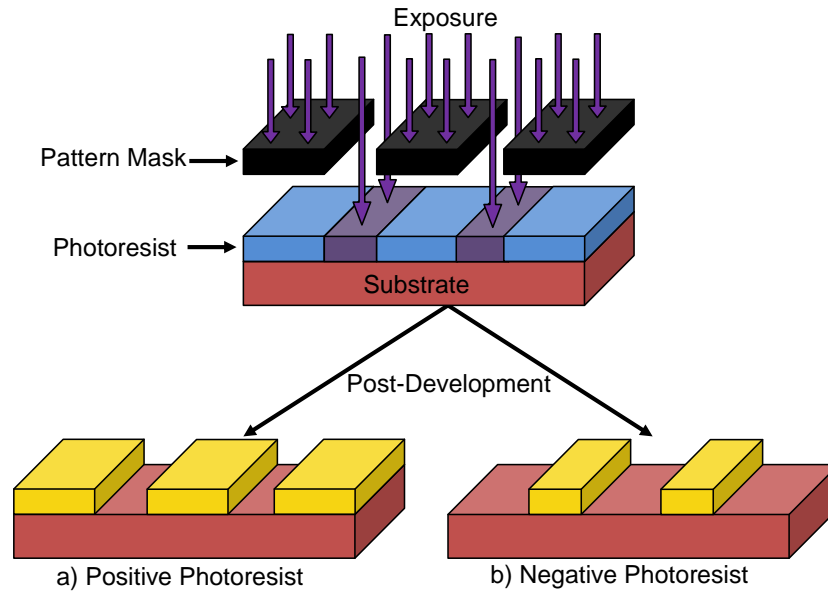


Fig. 2 a) Positive and b) negative PR structures during exposure and after development

Various mechanisms are used in UV exposure, but in the case of negative PRs such as the NR9-8000 used in this study, exposure to UV light causes breaks in the polymer chains and changes the chemistry of the PR. Although the PR is not physically broken down by the exposure, it allows for chemical differentiation between exposed and nonexposed areas by either promoting or inhibiting solubility in a developer solution. Exposure time can be used to modify sidewall profiles, which is a crucial element in some PR removal processes. Exposure of a PR material is usually measured as exposure dose and is defined as

$$Exposure = I \times t, \quad (1)$$

where t represents time (measured in seconds), and I represents light intensity (measured in milliwatts per square centimeter [mW/cm²]). The exposure of a PR is prescribed by the thickness (in microns) of the exposed area and the calculated sensitivity of the PR chemical.

After exposure, a postexposure bake step using a hot plate or oven heating is used to complete the chemical transformations initiated by the UV exposure. In this step, broken polymer chains can cross-link and form chains that are insoluble to a specific developing solution. The samples can then be immersed in the developer solution that removes the soluble resist while maintaining the insoluble areas prescribed by the pattern mask.³ The development and exposure steps are coupled parameters, meaning that increasing variation of time in both parameters affects the resulting feature details and sidewall profiles of the resulting PR. Optimization studies have often focused on the relationship between these 2 parameters to find a processing window in which the desired structures can be produced.^{1,4,5}

1.2 Coating and Removal Techniques

After PR pattern structures are successfully fabricated on a surface, there are 2 main options of processing and removal of the PR: lift-off and etch-removal techniques. These processing techniques, illustrated in Fig. 3, are part of what make photolithography a versatile technique in high-precision fabrication of 3-dimensional structures.

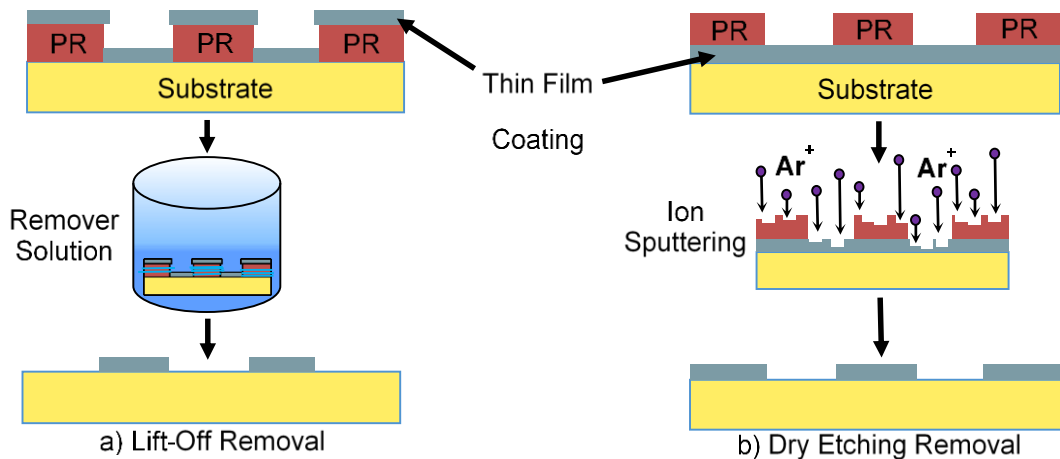


Fig. 3 Comparison of a) lift-off and b) dry-etching PR removal techniques. While lift-off uses solution to remove PR from the substrate, etching techniques dissolve a uniform top layer of material, both PR and metal.

Etch removal refers to a breakdown of both the PR and exposed underlying material layer, and can be accomplished by chemical or physical methods often referred to as wet- and dry-etching removal techniques, respectively. Chemical or wet-etching methods typically involve the use of solutions that contain strongly reactive chemicals such as hydrogen fluoride, ammonium hydroxide, or sulfuric acid to dissolve any exposed surface on the sample. Alternatively, dry-etching techniques such as sputter etching can be used to break down exposed surfaces with the bombardment of ionized gas atoms. As illustrated in Fig. 3b, etching removal methods breakdown any exposed surface, so PR materials can be used to selectively shield a patterned area of the sample, which yields a direct transfer of the PR pattern structure onto the underlying layer of material. This transfer is sometimes referred to as positive image transfer, but note that it is independent of the type of PR (positive or negative tone) that is used to create the pattern. Positive and negative tones refer to the PR type used to create structures and to the comparison of the patterning mask during UV exposure to the produced PR structures. Positive and negative pattern transfers refer to the methods of PR removal techniques, and correspond to the comparison of a PR structure pattern and the pattern that remains in the material after removal of the PR, as illustrated in Figs. 2 and 3.

Lift-off removal refers to a technique in which a coating is deposited over the PR structures and substrate, subsequently removed selectively by dissolving the PR, and leaving the negative image of the coating on the substrate, as illustrated in Fig. 3a. This technique has advantages over etching removal in that it does not require harsh chemical treatments or destructive bombardment of the substrate material. The chemical nature of PRs appropriate for lift-off removal usually results in structures that can only sustain a low-temperature environment exposure ($\sim 80\text{ C}^\circ$ – 120 C°) before breaking down, so etching PR techniques are still favored for patterns using high-processing-temperature materials. There are various methods of deposition for coating the surface of a PR, including thermal and electron beam evaporation, spin-coating, and sputter deposition. Because of the temperature restrictions, only materials and techniques with low processing temperatures can be used with these PRs. When using a PR for lift-off removal, it is important to produce a sidewall of resist structures that has an undercut profile. This profile, in addition to an appropriate choice of deposition technique, will create discontinuities in the coating material and assist in the successful pattern transfer during lift-off removal. If the sidewall profile has a straight or overcut profile, lift-off can be very difficult to achieve successfully, as shown in Fig. 4.

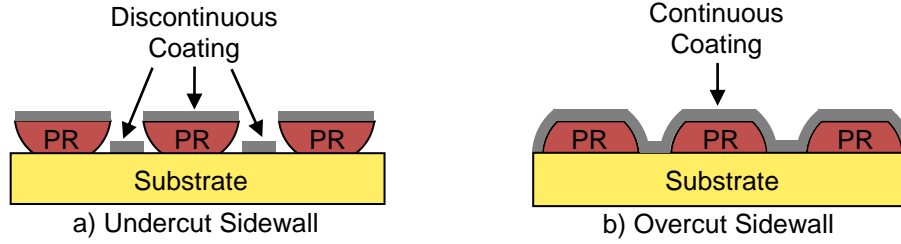


Fig. 4 Comparison of a) undercut sidewall profile that promotes coating discontinuities for easier lift-off and b) overcut sidewall profile

1.3 Processing Challenges

When establishing processing conditions for photolithography and PR removal, equipment and laboratory conditions must be taken into consideration. Ambient conditions, spin-coat setup, efficiency and uniformity of UV light source, target feature size, oven temperature distribution, and the reliability of coating techniques must all be taken into account to establish conditions that yield the desired PR structures with high quality and reproducibility. In this study, optimization of the processing parameters for Futurrex NR9-8000 negative-tone PR is systematically investigated for application in PR structures with feature sizes of 3–20 μm and appropriate sidewall profile for lift-off removal.

2. Methods

Systematic deviations were made from manufacturer-recommended PR processing conditions to investigate processing-structure relationships for the optimization of IDC fabrication, including PR response to manipulation of substrate material, spin speed, postexposure bake, exposure dose, and development process conditions. In all investigations, square substrates of silicon dioxide (SiO_2) (200 nm thick) on Si, each with an area of approximately 0.25 sq. inch. NR9-8000 negative-tone PR was coated by spin-coat application using the manufacturer-prescribed speed and duration for a range of target thicknesses including 6.5, 8.0, 9.0 and 16.5 μm . After spin-coating, all samples were soft-baked on a hot plate at 100 $^{\circ}\text{C}$ for 120 s, then exposed using a 365-nm-wavelength UV light source and either a “comb” pattern mask or the final IDC structure mask, which are illustrated in Fig. 5.

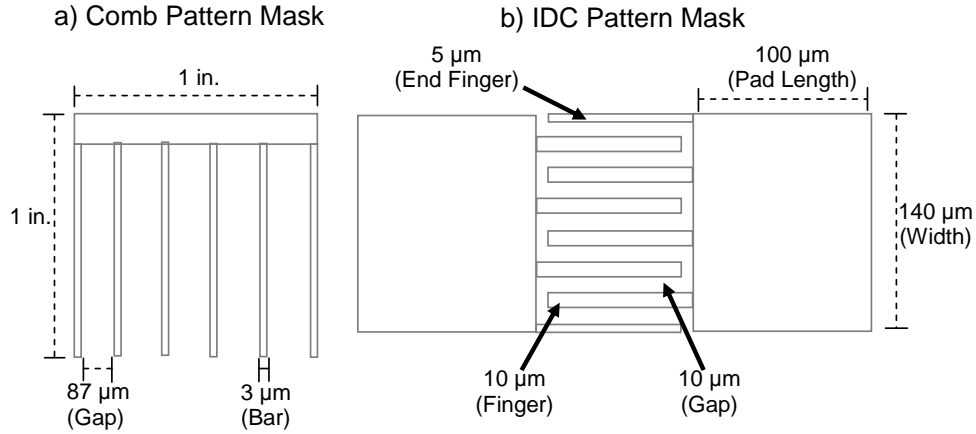


Fig. 5 a) Comb pattern and b) IDC pattern mask schematics with feature dimensions

To optimize the yield and feature resolution in the processed IDC structures, each step in the lithography process was investigated with variations to monitor the process as closely as possible. Obtaining cross-section images of the IDC fingers, which were important to image as the smallest aspect features of the PR structures, would have been an exceedingly difficult task using hand-scribing methods due to the 90- μm length of the structures. For these investigations, a modified pattern mask was used with a set of 1-inch-long, 3- μm -wide bars. This pattern had the advantages of having a smaller, yet still comparable feature size, and the 1-inch length of the structures made cross-section images much less difficult to obtain by hand-scribing methods.

After exposure, samples were returned to the hot plate for a postexposure bake at various temperatures and developed by immersion in an RD6 remover solution, followed immediately by 30 s of immersion and 10 s of rinsing using deionized water. After rinsing was completed, samples were dried with an N_2 gas source supplied through a handheld nozzle and scribed for cross-section scanning electron microscopy (SEM) imaging. Due to the high resistance of the samples, scribed SEM samples were coated with approximately 35 nm of platinum by direct current (DC) sputter deposition to avoid charging and increase SEM image fidelity.

2.1 Spin-Coat Study

Four spin-coating parameters were chosen to investigate the obtained PR thickness with respect to the manufacturer thickness ranges. For this study, a section of Kapton tape was placed across the SiO_2/Si substrate that would be removed after application of the PR to measure thickness by profilometry. The measurement setup is illustrated in Fig. 6.

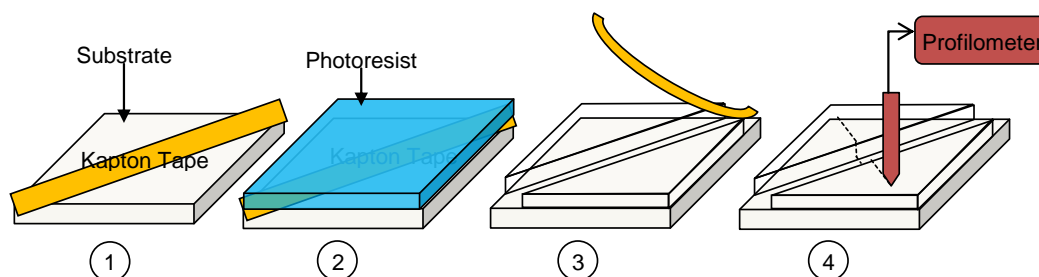


Fig. 6 Profilometry measurement setup for thickness measurement of as-applied PR layer prior to exposure and development processing: 1) apply Kapton tape, 2) spin-coat PR and soft-bake, 3) remove Kapton tape, and 4) measure step height

All samples were spin-coated for 40 s, with varying spinning speeds of 1,000, 2,000, 3,000, and 4,000 rpm. Samples were soft-baked to remove solvents and harden the PR prior to removal of the Kapton tape and measurement by profilometry. Comparisons of the film thickness after exposure and development processing were made by laser microscopy.

2.2 Postexposure Bake Study

Samples were processed with varying postexposure bake temperatures and investigated by laser microscope and cross-section SEM imaging with the following parameters:

- Spin-coat resists (4,000 rpm/40s; 6.5- μm target thickness)
- Soft-bake (150 °C for 120 s)
- Exposure (dose = 130 mJ/cm²)
- Postexposure bake (25 °C, 50 °C, 70 °C, 90 °C, and 110 °C/120 s)
- Development (17 s)

Sample thickness and sidewall profile were estimated by laser microscopy, and further inspection was made for 90 °C postexposure bake sample by cross-section SEM.

2.3 Development Time Study

Development time was studied using the following processing parameters:

- Spin-coat resists (3,000 rpm/40s; 8- μm target thickness)
- Soft-bake (150 °C/120 s)
- Exposure (dose = 130 mJ/cm²)

- Postexposure bake (100 °C/60 s)
- Development (34, 37, 40, 43, and 46 s)

All samples were coated with 35 nm of platinum by sputter deposition and examined by cross-section SEM for thickness and feature dimension variation.

2.4 Coating by Electron-Beam and DC Sputter Deposition

Electron beam (e-beam) and DC sputter deposition techniques were chosen for coating 2 μm of copper (Cu) at room temperature on the optimized PR structures. The investigations were made to assess the appropriate available methods for deposition of thick Cu coatings that would be used in IDC structures. After deposition, samples were compared using cross-section SEM imagery on the comb structures. For lift-off assessment, the IDC pattern mask was used, and structures were observed with optical microscopy to determine fidelity of fabricated features by both deposition methods.

3. Results and Discussion

3.1 Spin-Coat Study Results

Spin-coat speed variation after the soft-bake processing from 1,000 to 4,000 rpm was observed to correlate very well with the expected thickness dictated by the manufacture. The results are presented in Table 1. Although these results agreed after soft-bake processing, samples fabricated under similar conditions that were fully processed by exposure, postexposure baking, and development were observed by laser microscopy to contain only approximately 10%–20% of the original applied PR thickness remaining. This result suggested that the processing conditions after soft-baking were inappropriate and consistently causing the loss of approximately 80%–90% of the PR applied during spin-coating procedures.

Table 1. Expected PR thicknesses vs. measured thickness values after soft-bake and after development

Spin-coat Parameters (1,000 rpm/s)	Expected Thickness (μm)	Post-spin-coat Thickness (μm)	Postdevelopment Thickness (μm)
4/40	6.5–6.8	6.7	0.78
3/40	8.0–8.3	7.5	1.47
2/40	9.0–10.0	10.0	1.96
1/40	16.5–17.5	19.7	2.72

3.2 Postexposure Bake Study Results

The developed structures showed a large variation with all postexposure bake temperatures, with respect to overall thickness, sidewall profile, and even response of exposed versus unexposed areas of the PR during development. Using laser microscopy, structures were investigated and results can be seen in Fig. 7.

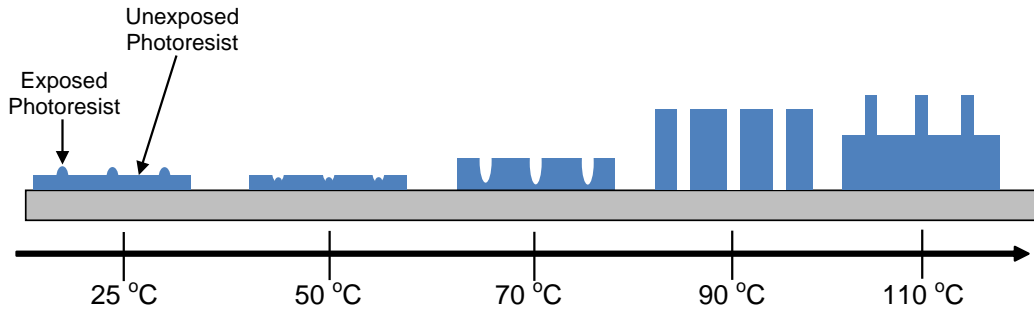


Fig. 7 PR profile after postexposure bake processing from room temperature to 110 °C

At room temperature, the exposed PR remained thicker than the unexposed areas, which suggests that without a postexposure bake, the exposed PR is less soluble in the developer solution. The samples at 90 °C and 110 °C both showed excellent structure, though at 110 °C there was a high degree of inhomogeneity in the structures observed, suggesting that longer development times may be needed with higher bake temperatures, which may be due to excess hardening of the PR during postexposure baking. A temperature of 100 °C was chosen for optimization, with a postexposure bake time of 60 s. The postexposure bake step was observed to be the most sensitive to variation of all the parameters investigated in this study.

3.3 Development Time Study Results

For an 8- μ m thickness PR with the previously listed exposure dose, development time was observed to be relatively insensitive to small variations (± 6 s), as seen in the comparison SEM micrographs in Fig. 8. Feature dimensions for all development times are also included in Table 2.

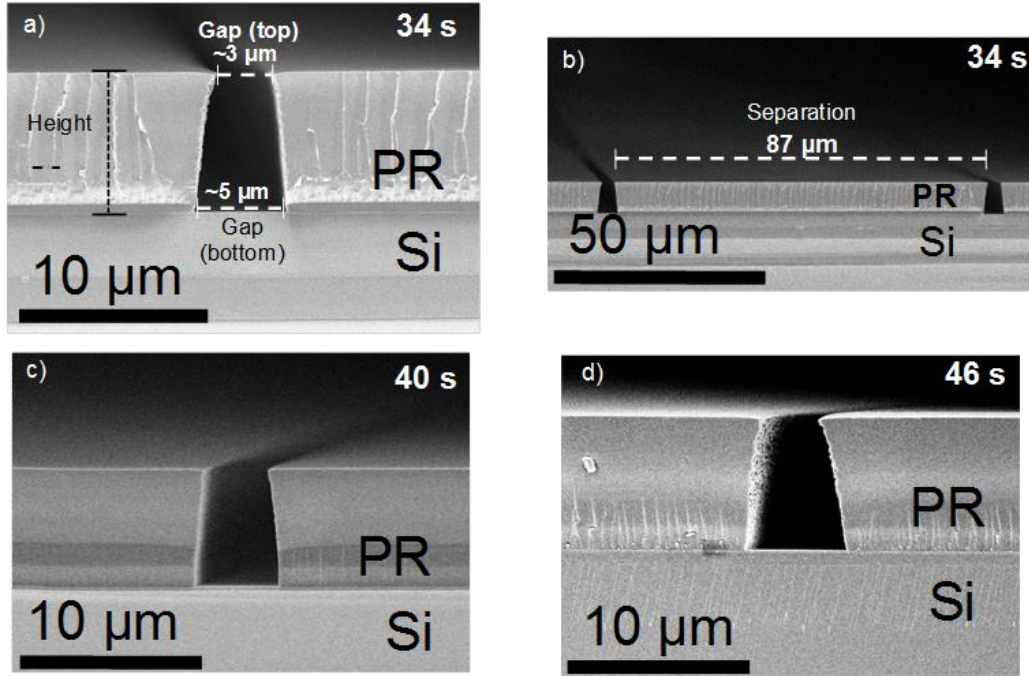


Fig. 8 Cross-section SEM micrographs of samples processed with 34-, 40-, and 46-s developer immersion durations

Table 2 Achieved feature dimensions for comb-mask pattern with variation of development duration

Develop Time (s)	Height (μm)	Gap Width, Top (μm)	Gap Width, Bottom (μm)	Separation Width (μm)
34	7.45	3.07	5.05	86.8
37	7.50	3.15	4.71	87.1
40	7.49	3.09	5.16	85.9
43	7.54	3.18	4.93	87.0
46	7.34	3.17	5.63	85.7

The optimized conditions for PR structures with 8-μm thickness processed on SiO₂/Si substrate were established as follows:

- Spin-coat resists (3,000 rpm/40s; 8-μm target thickness)
- Soft-bake (150 °C/120 s)
- Exposure (dose = 130 mJ/cm²)
- Postexposure bake (100 °C/60 s)
- Development (40 s immersion and gentle agitation)

3.4 Coating by E-Beam and DC Sputter Deposition Results

Deposition of 2 μm of Cu on both IDC and comb-pattern structures were conducted at room temperature, and cross-section SEM images revealed that sputter deposition caused a breakdown and major deformations of the PR structures, while the damage caused by e-beam coating of the same thickness was significantly less severe. SEM cross-sectional comparison of the structures are shown in Fig. 9.

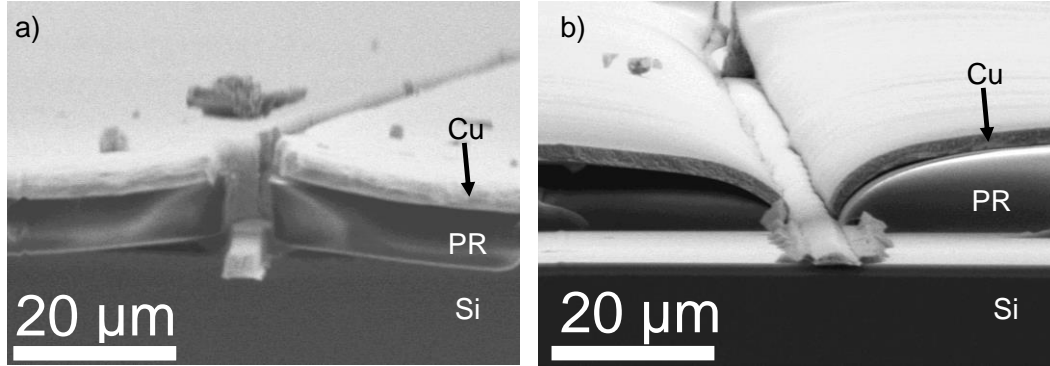


Fig. 9 SEM cross-section of PR structures after coating with 2 μm of Cu: a) e-beam deposition and b) sputter deposition

The PR structure damage caused by sputter deposition resulted in a destruction of the undercut profile desired for lift-off removal and caused anomalies at the edges of the Cu structures after lift-off was performed on the IDC pattern structures. For the comb-pattern structures, lift-off was only successful for the e-beam-deposited structures, while the structures deposited by DC sputter deposition seemed to be detached during lift-off. A comparison of the structures by optical microscopy is presented in Fig. 10.

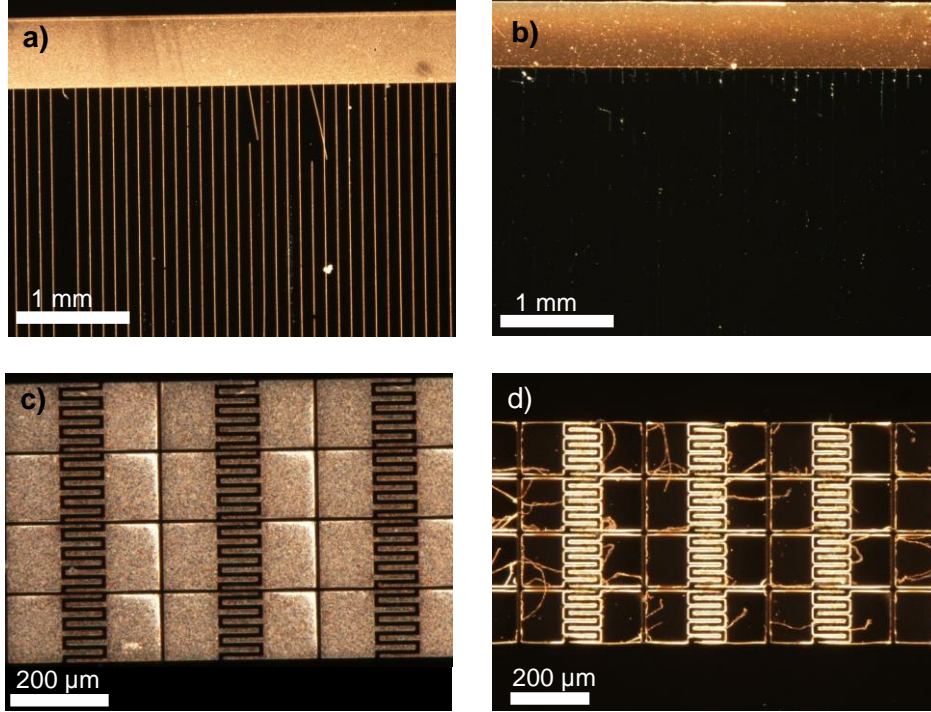


Fig. 10 Optical microscopy of Cu structures after lift-off removal of PR for a) comb pattern by e-beam, b) comb pattern by DC sputtering, c) IDC pattern by e-beam, and d) IDC pattern by DC sputtering

It seems that larger features where error of a few microns is permitted may be fabricated by DC sputtering, but the temperature increase and high-energy nature of the process makes it prohibitive for the smaller features. The results of this study suggest that e-beam deposition with a cooling source at the target should be used to avoid the high temperatures at which the NR9-8000 PR will begin to deform and break down.

4. Conclusions

Systematic variations were made to photolithography process for optimization of IDC structure fabrication. Results suggested that postexposure bake temperature was the most sensitive parameter to variation and a temperature of 100 °C produced the desired structures with an undercut profile that promoted discontinuities in an overlaying coating for greater success in lift-off removal procedures. It was observed by producing Cu coatings 2-μm thick on optimized PR structures that the high-energy nature of the DC sputter deposition process and high generated temperatures damaged PR structures and created anomalies in lift-off procedure results. This result suggests that e-beam deposition with a cooling source at the substrate is a more appropriate technique for the deposition of Cu coatings for IDC measurement applications using Futurrex NR9-8000 PR.

5. References

1. del Campo A, Greiner C. SU-8: a photoresist for high-aspect-ratio and 3D submicron lithography. *Journal of Micromechanics and Microengineering*. 2007;17:R81–R95.
2. Smith HI. A review of sub-micron lithography. *Superlattices and Microstructures*. 1986;2:129.
3. Grigorescu AE, Hagen CW. Resists for sub-20-nm electron beam lithography with a focus on HSQ: state of the art. *Nanotechnology*. 2009;20:292001.
4. Yoon JB, Han CH, Yoon E, Kim CK. A unified chemical bonding model for defect generation in a-SiH: photo-induced defects in photovoltaic devices and current-induced defects in TFTs. *Japanese Journal of Applied Physics Part 1, Regular Papers Short Notes and Review Papers*. 1998;37:7081.
5. Rathsack BM, Tabery CE, Scheer SA, Pochkowski M, Philbin C, Kalk F, Henderson CL, Buck PD, Willson CG. Optical lithography simulation and photresist optimization for photomask fabrication. In: Conley W, editor. *Microolithography 1999: advances in resist technology and processing XVI*; Mar 15–17; Santa Clara, CA. *Proceedings of SPIE* 1999; 1999 Jun. p. 1215–1226.

List of Symbols, Abbreviations, and Acronyms

DC	direct current
e-beam	electron beam
IDC	interdigitated capacitor
PR	photoresist
SEM	scanning electron microscopy
UV	ultraviolet

1 DEFENSE TECHNICAL
(PDF) INFORMATION CTR
DTIC OCA

2 DIRECTOR
(PDF) US ARMY RESEARCH LAB
RDRL CIO LL
IMAL HRA MAIL & RECORDS
MGMT

1 GOVT PRINTG OFC
(PDF) A MALHOTRA

5 DIR USARL
(PDF) RDRL WMM E
M COLE
S HIRSCH
C HUBBARD
M IVILL
E NGO

INTENTIONALLY LEFT BLANK.